Tracing the UV radiation with CN, HCN and CS molecules

A. Mirocha[1,2], *A. Karska*[2], *L. E. Kristensen*[3], *M. Gronowski*[4], *M. Figueira*[5], *M. Gładkowski*[2,6], *M. Żółtowski*[7], *Ł. Tychoniec*[8]

[1] Astronomical Observatory of the Jagiellonian University, ul. Orla 171, 30-244 Kraków, Poland
[2]Centre for Astronomy, Faculty of Physics, Astronomy and Informatics, Nicolaus Copernicus University, ul. Grudziądzka 5, 87-100 Toruń, Poland
[3]Centre for Star and Planet Formation, Niels Bohr Institute and Natural History Museum of Denmark, University of Copenhagen, Øster Voldgade 5-7, DK-1350 Copenhagen K, Denmark
[4]Institute of Physical Chemistry Polish Academy of Sciences, ul. Kasprzaka 44/52, 01-224 Warszawa, Poland
[5]National Centre for Nuclear Research, ul. Pasteura 7, 02-093 Warszawa, Poland
[6]Nicolaus Copernicus Astronomical Center, ul. Rabiańska 8, 87-100 Toruń, Poland
[7]University of Le Havre, Laboratoire Ondes et Milieux Complexes, UMR CNRS 6294,75 Rue Bellot, 76600 Le Havre, France
[8]Leiden Observatory, Leiden University, P.O. Box 9513, NL-2300RA Leiden, The Netherlands
amirocha@doctoral.uj.edu.pl

A newly-born protostar forms in a dense core deep inside a molecular cloud. The molecular cloud is characterised by high extinction in the optical range so observations at long wavelengths are necessary. Millimetre spectra include rotational lines of key molecules which are useful tracers of physics and chemistry around low-mass protostars. HCN, CN, and CS emission from the Serpens Main region is modelled using the radiative transfer code RADEX to determine the gas physical conditions and molecular abundances. This information provides input parameters to use in an astrochemical model in order to characterise the strength of the UV radiation. Thus, we gain a new understanding of chemical and physical processes around low-mass protostars.

Key words: stars: formation, ISM: individual objects: Serpens Main, ISM: molecules

INTRODUCTION

New discoveries of extrasolar planets trigger questions about star and planet formation and composition. Detailed studies on the earliest stages of stellar evolution are necessary in order to understand these phenomena. Protostars are formed in dense cores inside a molecular cloud. They can be classified by their bolometric luminosity for: low-mass protostars ($L_{\rm bol} < 10^2\,L_\odot$), intermediate-mass protostars ($10^2\,L_\odot - 10^4\,L_\odot$) and high-mass protostars ($L_{\rm bol} > 10^4\,L_\odot$). The earliest phases of star formation are characterised by gas and dust accretion from an envelope and bipolar, collimated outflows which transport molecular gas from the dense core ([1]). Protostars interact with their surroundings, changing chemical and physical properties of the matter in which the stars and planets form. In this turbulent environment, an energetic electromagnetic radiation, such as ultraviolet photons or X-rays, is produced which may ionise the environment of young stellar objects ([15]). The UV radiation field around high-mass protostars is estimated at 20-600 times higher than the average in the interstellar medium ([2]). The strength of the UV radiation around less massive young stellar objects is still a matter of debate.

The Serpens molecular cloud is characterised by a large sample of known protostars ([4]). At a distance of 436 ± 9 pc ([12]) it is one of the largest clouds containing low-mass protostars within 500 pc. The Serpens Main region is located in the northern part of the cloud. There are several low-mass protostars at a very early stage of their evolution. The initial identification of the protostars was obtained in the submillimetre range, hence the objects got numbered by their submillimetre luminosity with the SMM prefix.

OBSERVATIONS

The observations were obtained with the IRAM 30 telescope in 2009, between July 14 and 17, in good weather conditions. The observations were conducted with the Eight MIxer Receiver (EMIR) in the E090

Table 1: Overview of the observations

Mol.	Trans.	ν (GHz)	Beam size ($''$)	Beam eff. $\eta_{\rm MB}$
HCN	1-0	88.630416 88.631847 88.633936	28	0.81
CN	1-0	113.123369 113.170535 113.488142 113.490985 113.499643	22	0.78
CS	3-2	146.969029	16	0.74
$C^{34}S$	3-2	144.617109	16	0.74
$H^{13}CN$	1-0	86.338767 86.340184 86.342274	29	0.81
$H^{13}CN$	2-1	172.676573 172.677881 172.677959	14	0.68

Beam sizes and efficiencies are taken from `http://www.iram.es/IRAMES/mainWiki/Iram30mEfficiencies`

(73-117 GHz) and the E150 (125-184 GHz) bands and the VESPA correlator as the backend which allows us to obtain the spectra of the targeted lines: HCN, CN, CS and their isotopologues. Each spectrum (Fig.1) consists of 2800 channels with a velocity resolution of 0.1 km s^{-1}. Two $200'' \times 240''$ on-the-fly maps of the Ser-SMM1 region (centered at $\alpha_{\rm J2000} = 18^h29^m49.6^s$, $\delta_{\rm J2000} = +01°15'20.5''$) and the Ser-SMM3/Ser-SMM4 region (centered at $\alpha_{\rm J2000} = 18^h29^m56.6^s$, $\delta_{\rm J2000} = +01°14'00.3''$) were obtained. The observations were conducted using position-switching toward an emission-free reference position. The beam size varies from $14''$ for $H^{13}CN$ 2-1 to 29 arcsec for $H^{13}CN$ 1-0. A summary of the observations is presented in Tab. 1.

RESULTS AND CONCLUSIONS

The HCN molecule photodissociates into the CN radical in the presence of UV radiation while CN itself is less sensitive to photodissociation. Thus, the CN/HCN ratio is widely used as a tracer of the ultraviolet radiation (e.g. [5], [3], [13]). Fig. 2 shows the CN 1-0 to HCN 1-0 integrated intensity ratio over all observed hyperfine components performed above a 3σ level. In the studied region the highest I(CN)/I(HCN) ratio is co-spatial with the more evolved protostars: Ser-SMM5 and Ser-SMM6. These results show that the I(CN)/I(HCN) ratio can be a good tracer of more evolved protostars independent of a Spectral Energy Distribution analysis. A peak in I(CN)/I(HCN) ratio can also be found between Ser-SMM1 and Ser-SMM10 protostars. Recent interferometer studies ([7]) show that Ser-SMM1 is a multiple system. The peak in the I(CN)/I(HCN) ratio may originate from an outflow of one of the components. The HCN emission dominates toward molecular outflow positions as well as in denser regions with a large concentration of protostars, where the energetic radiation is mostly absorbed by the dust. The I(CN)/I(HCN) ratio is particularly low around Ser-SMM9, Ser-SMM4 and Ser-SMM10.

The CN, HCN and CS abundances can be calculated based on the intensities of the observed molecular lines using the RADEX radiative transfer code ([16]). We prepared the sets of RADEX models for the following envelope parameters: kinetic temperature of 50 K and hydrogen densities varying from 10^3 to 10^6 cm^{-3}. A temperature of 50 K is chosen as an average value for a protostar envelope temperature profile calculated for Ser-SMM1 and Ser-SMM4 ([9]). Three the strongest hyperfine components of the CN 1-0 line (F=3/2→1/2, F=5/2→3/2, F=1/2→1/2) were used to determine optical depths. Recent studies show anomalies in the hyperfine components ratio of the HCN 1-0 line ([11]), thus the opacity was calculated based on the HCN 1-0/$H^{13}CN$ 1-0 abundances ratio. The HCN/$H^{13}CN$ ratio was adopted as 67 ([18]) and the ratios between hyperfine components of CN as 0.1235:0.3333:0.0988 ([14]). Depending on the source,

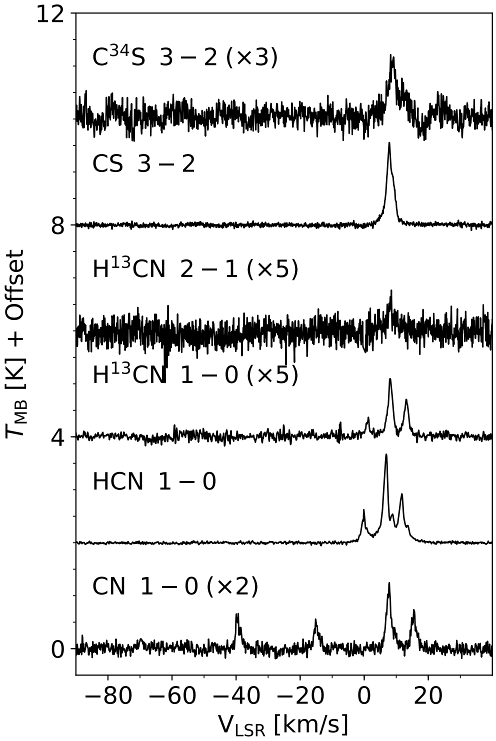

Fig. 1: Averaged spectra of $C^{34}S$ 3-2, CS 3-2, $H^{13}CN$ 2-1, $H^{13}CN$ 1-0, HCN 1-0 and CN 1-0 lines observed in the Serpens Main region. CN and HCN hyperfine splitting components are displayed as described in Tab. 1.

the CN lines opacity varies from 0.3-5.7, and the HCN 1-0 - between 0.64-10.31. The lines opacity is particularly large at Ser-SMM1, Ser-SMM5 and Ser-SMM12 positions. Even though the absolute column densities may be underestimated in positions where we have an optically thick emission, it should not affect the $N(\mathrm{CN})/N(\mathrm{HCN})$. The RADEX models show that the $N(\mathrm{CN})/N(\mathrm{HCN})$ ratio around low-mass protostars varies between 1 and 10 regardless of molecular hydrogen density. The $N(\mathrm{CN})/N(\mathrm{CS})$ ratio varies between 10 and 30 for all of the protostellar positions, while the $N(\mathrm{CS})/N(\mathrm{HCN})$ ratio ranges from 0.1 to 0.3. An exemplary set of models is shown in Fig. 3.

The astrochemical model of Nahoon ([19]) together with the kida.uva.2014 database ([20]) were used in modelling the chemical evolution of the cloud. The astrochemical database kida.uva.2014 contains a list of reactions together with parametrised reaction rate constants. A reaction rate depends on the temperature. However, the chemical evolution depends also on several parameters, including UV radiation flux and the cloud density, as well as dust grain size and abundance. Our model is a nearly pure gas-phase model. It contains 489 species and 7509 reactions with 13 gas-grain reactions. Our network contains only two classes of grain-related reactions, namely: i) between negatively charged grains and atomic cations ii) between neutral grains and electrons. The model was run in two steps. Firstly, we modelled the starless, dense molecular cloud with typical parameters of $n_{\mathrm{HI+2\dot{H}_2}} = 10^4$ cm^{-3}, $T = 10$ K, $A_{\mathrm{V}} = 5$ mag. The abundances of chemicals obtained at time 10^6 years were the initial parameters for a set of models differing by temperature, density, and UV field intensities. This time we modelled the closest environment of a low-mass protostar. The abundance ratios of interesting molecules do not change dynamically at low temperatures which allowed us to fix the temperature parameter at 50 K, which is a typical temperature for a protostar's envelope. Comparing the $n(\mathrm{CN})/n(\mathrm{HCN})$ results with similar plots of $n(\mathrm{CN})/n(\mathrm{CS})$ (Fig. 4 and Fig. 5), we restrict the parameter space to very-low-density and weakly irradiated gas. Astrochemical models computed for the $n(\mathrm{CS})/n(\mathrm{HCN})$ ratio show similar behaviour. At the protostellar positions high hydrogen densities ($\approx 10^6$ cm^{-3}) can be assumed. The models allow estimating the strength of needed UV radiation field in terms of Habing units $\mathrm{G_0}$, where 1 $\mathrm{G_0}$ equals a flux of 1.6×10^{-3} erg cm^{-2} s^{-1}, integrated over the energy range 6 – 13.6 eV ([6]). The background UV radiation is absorbed deep in dense clouds, where protostars are formed. Thus, UV radiation descripted by our models is produced around protostars. The models show that

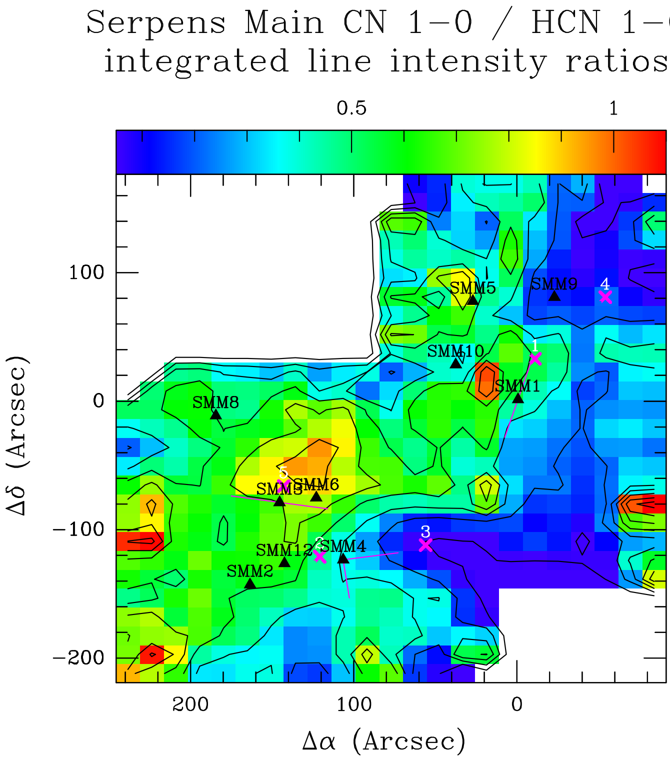

Fig. 2: Integrated CN/HCN 1-0 ratios in the Serpens Main region. Black triangles show the positions of the protostars, whereas purple lines show the associated outflow directions. Outflow positions are displayed as purple crosses. The map is centered at the SMM1 position ($\alpha_{\rm J2000} = 18^h29^m49.6^s$, $\delta_{\rm J2000} = +01°15'20.5''$).

$G_0 \approx 0.03$ is needed to cover the observations.

Recent studies showed non-zero UV radiation in outflow cavities of young stellar objects (e.g. [17], [10], [8]). These results are confirmed with the astronomical model of Nahoon in the gas of 50 K at the positions of low-mass protostars. A radiation source of a few hundredth of the average interstellar UV radiation field is required to explain the observational ratios. The presence of energetic particles changes chemical and physical properties of the closest surroundings of low-mass protostars.

ACKNOWLEDGEMENT

AM, AK and MG acknowledge support by the Polish National Science Center grant 2016/21/D/ST9/01098. The research was conducted as a part of the InterAPS project of the Polish National Agency of Academic Exchange.

This work is based on observations carried out with the IRAM 30m telescope. IRAM is supported by INSU/CNRS (France), MPG (Germany) and IGN (Spain).

This research has made use of data from the Herschel Gould Belt survey (HGBS) project (http://gouldbelt-herschel.cea.fr). The HGBS is a Herschel Key Programme jointly carried out by SPIRE Specialist Astronomy Group 3 (SAG 3), scientists of several institutes in the PACS Consortium (CEA Saclay, INAF-IFSI Rome and INAF-Arcetri, KU Leuven, MPIA Heidelberg), and scientists of the Herschel Science Center (HSC).

REFERENCES

[1] Arce, H. G. & Sargent, A. I. 2006, ApJ, 646, 1070
[2] Benz, A. O., Bruderer, S., van Dishoeck, E. F.;, et al. 2016, A&A, 590, 105
[3] Chapillon, E., Guilloteau, S., Dutrey, A., et al. 2012, A&A, 537, A60
[4] Evans, Neal J., I., Dunham, M. M., Jørgensen, J. K., et al. 2009, ApJS, 181, 321

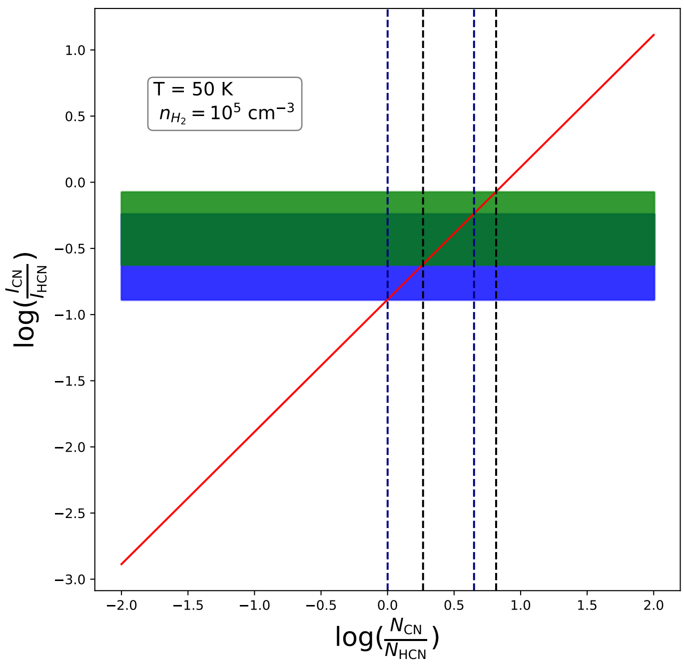

Fig. 3: $N(\mathrm{CN})/N(\mathrm{HCN})$ column density ratio for $n_{\mathrm{H_2}} = 10^5$ cm^{-3} and $T_{\mathrm{kin}} = 50$ K (red line). The observed line intensity ratio is plotted in green (protostellar positions) and blue (outflow positions). $N(\mathrm{CN})/N(\mathrm{HCN})$ corresponding to the observed $I(\mathrm{CN})/I(\mathrm{HCN})$ is marked with dashed, vertical lines.

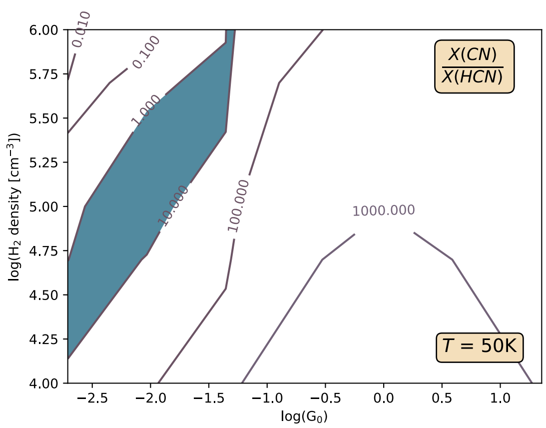

Fig. 4: Contour plot of Nahoon sets of models of CN/HCN abundance ratios with T = 50 K against UV radiation flux ($\mathrm{G_0}$ parameter) and hydrogen densities. The observational abundances ratio is represented by the blue area. An additional UV radiation of a few hundredth of the average interstellar UV radiation flux is enough to cover the observations in wide range of total hydrogen densities.

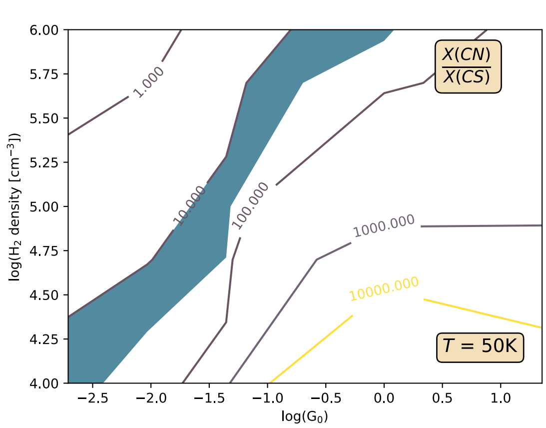

Fig. 5: Similar to Fig. 4 but for CN/CS abundances ratios.

[5] Fuente, A., Martin-Pintado, J., & Gaume, R. 1995, ApJ, 442, L33
[6] Habing, H. J. 1968, Bull. of the Astron. Inst. of the Neth., 19, 421
[7] Hull, Ch. L. H., Girart, J. M., Tychoniec, Ł., et al., 2017, ApJ, 847, 13
[8] Karska, A., Kaufman, M. J., Kristensen, L. E., et al. 2018, ApJS, 235, 45
[9] Kristensen, L. E., van Dishoeck, E. F., van Kempen, T. A., et al. 2010, A&A, 516, 16
[10] Kristensen, L. E., van Dishoeck, E. F., Mottram, J. C., et al. 2017, A&A, 605, 19
[11] Loughnane, R. M., Redman, M. P., Thompson, M. A., et al. 2012, MNRAS, 420, 1367
[12] Ortiz-León, G. N., Dzib, S. A., Kounkel, M. A., et al. 2017, ApJ, 834, 143
[13] Riaz, B., Thi, W. F., & Caselli, P. 2018, MNRAS, 481, 4662
[14] Skatrud, D. D., De Lucia, F. C., Blake, G. A., et al. 1983, Journal of Molecular Spectroscopy, 99, 35
[15] Stäuber, P., Benz, A. O., Jørgensen, J. K., et al. 2007, A&A, 466, 977
[16] van der Tak, F. F. S., Black, J. H., Schöier, et al. 2007, A&A, 468, 627
[17] van Kempen, T. A., van Dishoeck, E. F., Güsten, R., et al., 2009, A&A, 501, 633
[18] Yan, Y. T., Zhang, J. S., Henkel, C., et al. 2019, ApJ, 877, 15
[19] Wakelam, V., Herbst, E., Loison, J. C., et al. 2012, ApJS, 199, 21
[20] Wakelam, V., Loison, J. C., Herbst, E., et al. 2015, ApJS, 217, 7